

High-Content Assay Multiplexing for Toxicity Screening in Induced Pluripotent Stem Cell-Derived Cardiomyocytes and Hepatocytes

Fabian Alexander Grimm,^{1,*} Yasuhiro Iwata,^{1,*} Oksana Sirenko,² Michael Bittner,³ and Ivan Rusyn¹

¹Department of Veterinary Integrative Biosciences, College of Veterinary Medicine and Biomedical Sciences, Texas A&M University, College Station, Texas.

²Molecular Devices, LLC, Sunnyvale, California.

³Translational Genomics Research Institute, Texas A&M University, College Station, Texas.

*These authors contributed equally to this work.

ABSTRACT

Cell-based high-content screening (HCS) assays have become an increasingly attractive alternative to traditional *in vitro* and *in vivo* testing in pharmaceutical drug development and toxicological safety assessment. The time- and cost-effectiveness of HCS assays, combined with the organotypic nature of human induced pluripotent stem cell (iPSC)-derived cells, open new opportunities to employ physiologically relevant *in vitro* model systems to improve screening for potential chemical hazards. In this study, we used two human iPSC types, cardiomyocytes and hepatocytes, to test various high-content and molecular assay combinations for their applicability in a multiparametric screening format. Effects on cardiomyocyte beat frequency were characterized by calcium flux measurements for up to 90 min. Subsequent correlation with intracellular cAMP levels was used to determine if the effects on cardiac physiology were G-protein-coupled receptor dependent. In addition, we utilized high-content cell imaging to simultaneously determine cell viability, mitochondrial integrity, and reactive oxygen species (ROS) formation in both cell types. Kinetic analysis indicated that ROS formation is best detectable 30 min following initial treatment, whereas cytotoxic effects were most stable after 24 h. For hepatocytes, high-content imaging was also used to evaluate cytotoxicity and cytoskeletal integrity, as well as mitochondrial integrity and the potential for lipid accumulation. Lipid accumulation, a marker for hepatic steatosis, was most reliably detected 48 h following treatment with test

compounds. Overall, our results demonstrate how a compendium of assays can be utilized for quantitative screening of chemical effects in iPSC cardiomyocytes and hepatocytes and enable rapid and cost-efficient multidimensional biological profiling of toxicity.

INTRODUCTION

To date, toxicity testing of pharmaceutical and industrial chemicals, as well as environmental agents, relies primarily on data derived from animal studies. While *in vivo* models are still widely regarded as the most acceptable testing systems for regulatory decision making, the low throughput, high costs, regulatory pressure, and the limited predictability of human biological responses have led to the reduction of animal use being a primary goal in toxicology.¹⁻³ However, these challenges welcome new opportunities for novel *in vitro* and computational technologies as feasible alternatives to traditional animal testing. A promising solution to overcome the limitations of traditional toxicity testing lies in emerging high-throughput screening (HTS) technologies to complement and potentially replace *in vivo* testing.⁴ Current federal initiatives to improve acceptance of HTS data in regulatory decision-making include the Tox21 and ToxCast programs.^{5,6} Likewise, HTS is widely applied in pharmaceutical drug development to improve selection criteria to prioritize lead molecules for animal testing.⁷

HTS can be broadly divided into two categories: biochemical assays and cell-based assays.^{8,9} While biochemical assays are easily accessible, data interpretation is usually target specific.⁸ To date, cell-based HTS assays rely primarily on the use of tumor-derived and primary cell lines and cover relatively narrow biological phenotypes, such as cell proliferation and/or cytotoxicity. Consequently, there is a considerable demand to increase both physiological relevance and multidimensionality of HTS assays.

Recent breakthroughs in stem cell technologies have resulted in the development and widespread availability of

© Grimm et al. 2015; Published by Mary Ann Liebert, Inc. This Open Access article is distributed under the terms of the Creative Commons Attribution Noncommercial License (<http://creativecommons.org/licenses/by-nc/4.0/>) which permits any noncommercial use, distribution, and reproduction in any medium, provided the original author(s) and the source are credited.

induced pluripotent stem cell (iPSC)-derived cell types, organotypic cell culture models that resemble their somatic counterparts both genetically and physiologically.^{10,11} In fact, human iPSC-derived two- and three-dimensional culture systems are considered to be highly physiologically relevant and hold promise to overcome the limitations associated with traditional cell lines and primary cells.¹⁰ A number of studies have indicated the potential for iPSC cardiomyocytes and hepatocytes to replicate cell-specific adverse effects of test chemicals.^{12–14} iPSC cardiomyocytes are a particularly attractive *in vitro* model system due to their use for evaluation of cardiac function, a challenging phenotype to model even in animals.¹⁵ Likewise, iPSC hepatocytes retain metabolic capacity on par with primary hepatocytes.¹⁶

A major challenge for regulatory acceptance of the data from HTS assays is in ensuring that tissue- and pathway-specific effects of chemicals can be captured. For example, cardiotoxicity and hepatotoxicity can be induced by a variety of mechanisms, including reactive oxygen species (ROS) formation, mitochondrial dysfunction, and disorders of lipid metabolism.^{17–20} Thus,

simultaneous detection of various phenotypes through multidimensional combination of high-content screening (HCS) assays can provide valuable orthogonal information on a variety of tissue- and pathway-specific endpoints.^{21,22}

This study used iPSC cardiomyocytes and hepatocytes to demonstrate the potential of a variety of HCS assay combinations for testing the potential toxicity of chemicals and complex substances (Fig. 1). The overall aim was to improve *in vitro* toxicity testing by reducing the time and cost of the assays while enhancing the mechanistic interpretation of the readouts so that confidence in animal replacement tests is improved. In particular, we demonstrate that intracellular calcium flux measurements to assess effects on cardiomyocyte contractility can be successfully combined with a competitive ELISA to determine G-protein-coupled receptor (GPCR) activation, a mechanism by which cardiotoxic compounds can induce chronotropic effects. Moreover, we applied high-content imaging to simultaneously capture effects on cell viability, mitochondrial integrity, and ROS formation in iPSC-derived cardiomyocytes and hepatocytes. We also demonstrate that imaging can be applied to assess cytoskeletal

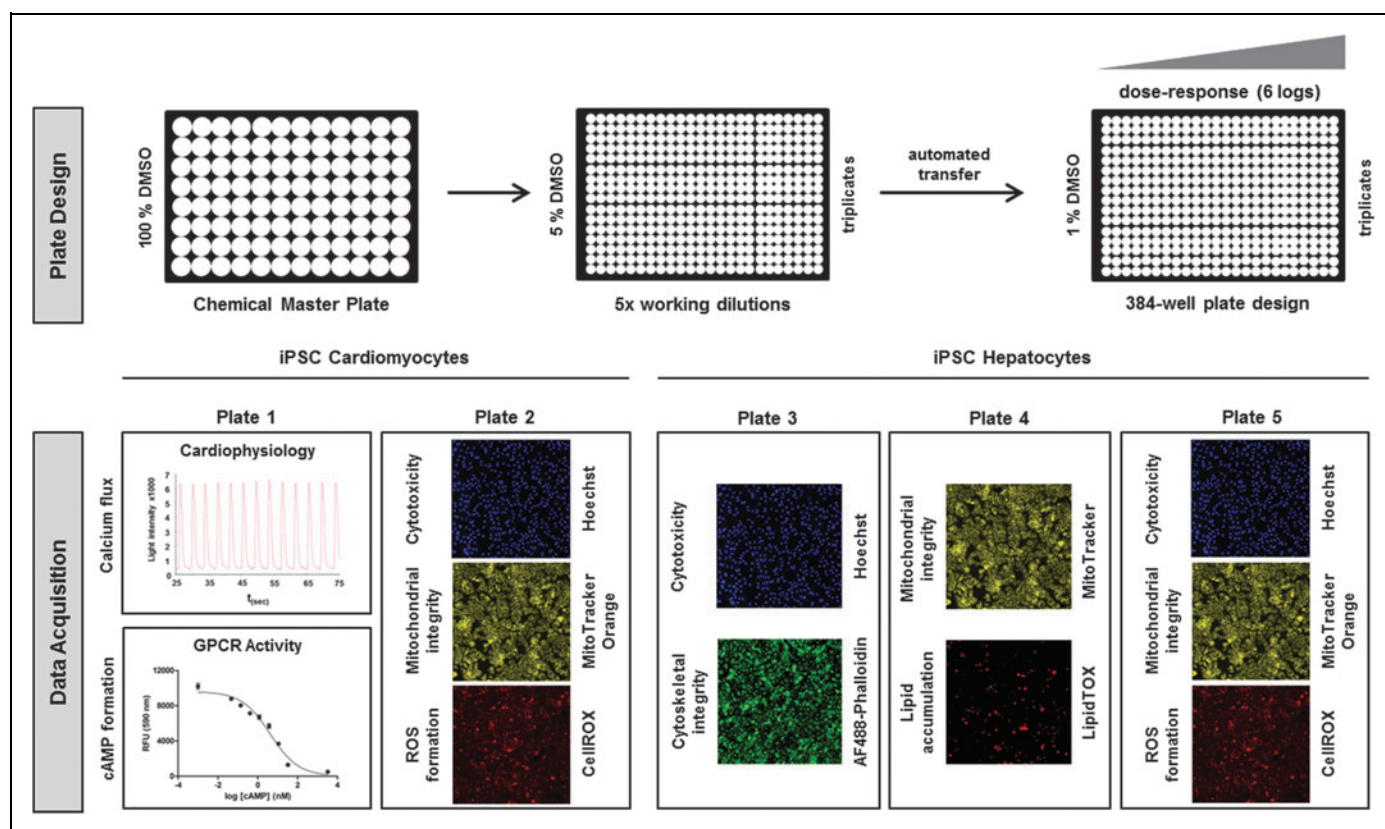


Fig. 1. Assay plexing for multidimensional toxicity screening of iPSC-derived cardiomyocytes and hepatocytes. In this study, we present a combinatorial approach to comprehensively assess cardiotoxic and hepatotoxic effects of test chemicals *in vitro* through screening of cardiophysiological effects (calcium flux and GPCR activity assays, plate 1) and high-content imaging-based determination of cytotoxicity, mitochondrial integrity, ROS formation, cytoskeletal integrity, and lipid accumulation (plates 2–5). GPCR, G-protein-coupled receptor; iPSC, induced pluripotent stem cell; ROS, reactive oxygen species.

integrity and lipid accumulation, an indicator of hepatocellular steatosis, in iPSC-derived hepatocytes.

MATERIALS AND METHODS

Chemicals and Biologicals

iCell Cardiomyocytes (Catalog No. CMC-100-010-001; Lot No. 1031999) and Hepatocytes (Catalog No. PHC-100-020-001; Lot No. 1636 and 1208), including plating and maintenance media, were purchased from Cellular Dynamics International (Madison, WI). EarlyTox Cardiotoxicity Kits, including reference standards isoproterenol, propranolol, and sotalol, and CatchPoint cAMP GPCR assay kits were purchased from Molecular Devices, LLC (Sunnyvale, CA). B-27 medium supplement, CellROX Deep Red reagent, gentamicin (50 mg/mL), Hank's Balanced Salt Solution, HCS LipidTOX Deep Red reagent, Hoechst 33342, MitoTracker Orange CMTMRos reagent, penicillin/streptomycin solution, and RPMI 1640 medium were obtained from Life Technologies (Grand Island, NY). 3-Isobutyl-1-methylxanthine, amiodarone hydrochloride, cisapride monohydrate, crizotinib, doxorubicin hydrochloride, formaldehyde solution, forskolin, Krebs-Ringer bicarbonate buffer (KRBG), sodium bicarbonate, and tetraoctylammonium bromide (TAB) were all obtained from Sigma-Aldrich (St. Louis, MO). Dimethyl sulfoxide (DMSO), dexamethazone, hydrogen peroxide (3%), menadione, recombinant oncostatin M, and sunitinib were purchased from Fisher Scientific (Waltham, MA).

Cardiomyocyte Cell Culture

iCell Cardiomyocytes were plated and maintained in tissue culture-treated 384-well plates according to instructions provided by Cellular Dynamics International. Microplates were prepared by adding 25 μ L of a 0.1% (w/v) gelatin solution per well and subsequent incubation for 2 h at 37°C and 5% CO₂. Vials containing iCell Cardiomyocytes were removed from vapor phase liquid nitrogen storage immediately before plating and thawed for 4 min in a water bath at 37°C. The contents of a single vial were then resuspended in a total of 10 mL plating medium containing 1:500 (v/v) penicillin/streptomycin solution at room temperature. Cell density of the suspension was routinely tested by microscopic analysis of trypan blue-stained cells using disposable hemocytometers. Based on the determined cell density, the cell suspension was diluted in plating medium to provide a final cell concentration of 2×10^5 viable cells/mL. Subsequently, the gelatin solution was aspirated from the microplate and 25 μ L of cell suspension was added per well, resulting in an estimated cell density of 5,000 viable cells/well. Plates were kept at room temperature for ~30 min before they were incubated at 37°C and 5% CO₂. Forty-eight hours following cell seeding, the plating medium was exchanged with 30 μ L of maintenance medium

containing 1:500 penicillin/streptomycin. Maintenance medium was subsequently changed every other day for 12 days. On the evening before an experiment, the medium was exchanged and replaced by 25 μ L of fresh medium.

Hepatocyte Cell Culture

iCell Hepatocytes were plated and maintained in collagen I-coated 384-well plates according to instructions provided by Cellular Dynamics International. Briefly, cryopreserved iCell hepatocytes were thawed for 3 min in a water bath at 37°C. After thawing, cells were resuspended in plating medium [RPMI containing 0.1 μ M dexamethasone, 2% (v/v) B27 supplement, 25 μ g/mL gentamicin, 20 ng/mL oncostatin M, and 2% (v/v) iCell Hepatocyte medium supplement] to yield a final cell density of 7.2×10^5 cells/mL. As for cardiomyocytes, cell density and viability were assessed using the trypan blue exclusion test. Twenty-five microliters of cell suspension was plated per well, resulting in a theoretical plating density of 1.8×10^4 viable cells/well, and plates were incubated at room temperature for ~30 min before they were incubated at 37°C and 5% CO₂. Plating medium was replaced after the first 4 h and subsequently every day for 4 days. Four days following cell seeding, the plating medium was exchanged with 25 μ L/well maintenance medium (RPMI, 0.1 μ M dexamethasone, 2% (v/v) B27 supplement, 25 μ g/mL gentamicin, and 2% (v/v) iCell hepatocyte medium supplement). Maintenance medium was replaced every other day until the day of measurements.

Preparation of Test Chemicals and Treatment of iCell Cardiomyocytes and Hepatocytes

Test chemicals were prepared as 100 \times concentrated stocks in pure DMSO and serially diluted in either log or semilog format. In addition, samples of two commercial gas oils were prepared by extracting 5 mL of a gas oil into 20 mL DMSO using the American Society for Testing and Materials standard procedure.²³ Following solvent evaporation, the extract was weighed and subsequently resolubilized in 4 mL DMSO. Chemical master plates were stored at -20°C until further use. On the day of the experiment, master plates were thawed and 5 μ L of each sample was diluted into 95 μ L of the medium per well in a 384-well 5 \times concentrated working solution plate. Dilutions of each concentration were prepared in triplicate. These working solution plates were equilibrated at 37°C and 5% CO₂ before appropriate volumes were transferred to the assay plates.

Calcium Flux Measurements

Calcium flux in cardiomyocytes was assessed using the instructions provided by the EarlyTox Cardiotoxicity Kit from Molecular Devices, LLC (Table 1). Briefly, cells in 25 μ L medium per well were equilibrated for 2 h at 37°C in the presence

Table 1. Calcium Flux and GPCR Activity Measurements in iPSC Cardiomyocytes

Step	Parameter	Value	Description
1	Dispense gelatin solution	25 μ L	0.1% Gelatin in water
2	Incubation time	2 h	37°C
3	Plate cells	25 μ L	5.0×10^3 iCell cardiomyocytes
4	Incubation time	12 days	37°C, 5% CO ₂
5	Change media	25 μ L	Every other day
6	Dispense 2 \times staining solution	25 μ L	EarlyTox Cardiotoxicity Kit
7	Incubation time	2 h	37°C, 5% CO ₂
8	Reading	Ex: 470–495 nm, Em: 515–575 nm	FLIPR Tetra [®]
9	Library compounds	12.5 μ L	5 \times Conc. stock
10	Incubation time	10, 30, 60, 90 min	37°C, 5% CO ₂
11	Reading	Ex: 470–495 nm, Em: 515–575 nm	FLIPR Tetra
12	Wash	Once	With KRBG
13	Dispense stimulation buffer	15 μ L	0.75 mM IBMX in KRBG
14	Incubation time	10 min	37°C, 5% CO ₂
15	Dispense buffer control or positive control	7.5 μ L	PBS or 3 \times forskolin
16	Incubate	15 min	37°C, 5% CO ₂
17	Dispense lysis buffer	7.5 μ L	CatchPoint cAMP Fluorescent Assay Kit
18	Incubation time	10 min	Room temperature, shaking plates
19	Dispense cell lysate or cAMP calibrator	20 μ L	CatchPoint cAMP Fluorescent Assay Kit
20	Dispense anti-cAMP antibody working solution	20 μ L	CatchPoint cAMP Fluorescent Assay Kit
21	Incubation time	5 min	Room temperature
22	Dispense horseradish peroxidase-cAMP conjugate	20 μ L	CatchPoint cAMP Fluorescent Assay Kit
23	Incubation time	2 h	Room temperature
24	Wash	Four times, 80 μ L	CatchPoint cAMP Fluorescent Assay Kit
25	Dispense substrate solution	50 μ L	CatchPoint cAMP Fluorescent Assay Kit
26	Incubation time	10 min	Room temperature, in the dark
27	Reading	Ex: 470–495 nm, Em: 515–575 nm	FLIPR Tetra

Step Notes

1. Plate: black, clear bottom 384-well plate (No. 353962; Corning, NY).
3. Remove gelatin solution before plating cells.
5. For cell maintenance, 25 μ L of medium was exchanged every other day. On the evening before the experiment, old medium was replaced with 25 μ L fresh medium.
9. Final DMSO concentration on assay plate: 1%.
12. KRBG: Krebs-Ringer bicarbonate buffer with glucose, pH 7.4.
13. IBMX: 3-isobutyl-1-methylxanthine.
15. Thrice forskolin: 60 μ M in PBS (final concentration: 20 μ M).
19. Dispense samples to a 384-well plate coated with goat anti-Rabbit IgG.

DMSO, dimethyl sulfoxide; GPCR, G-protein-coupled receptor; iPSC, induced pluripotent stem cell; PBS, phosphate-buffered saline.

of 25 μL of prewarmed calcium dye reagent. Before treatment with test chemicals, basal calcium flux was recorded at 515–575 nm following excitation at 470–495 nm for 100 s in 0.125 s read intervals using the FLIPR tetra plate reader (Molecular Devices). The exposure time per read was 0.05 s, the gain was set to 2,000, and the excitation intensity was set to 30%. The instrument temperature was kept at a constant 37°C. Test chemicals (12.5 μL of 5 \times concentration working solutions) at the appropriate concentrations were added simultaneously to all wells using the instrument-specific automated liquid handler. Between subsequent readings at 10, 30, 60, and 90 min, cells were incubated at 37°C and 5% CO_2 .

Preparation of Cell Lysates for GPCR Activity Assay

Following completion of calcium flux measurements, media containing calcium dye were aspirated and cardiomyocytes were washed with 80 μL of KRBG (pH 7.5) before 15 μL of stimulation buffer (KRBG containing 800 nM IBMX) was added (Table 1). After 10 min of incubation at room temperature, 7.5 μL of either phosphate-buffered saline (PBS) (sample wells and negative controls) or 60 μM forskolin in PBS (positive controls) was added. Cells were incubated for 15 min at 37°C before the addition of 7.5 μL of lysis buffer (supplied as part of the CatchPoint GPCR assay kit). Microplates were then gently mixed on a plate shaker for 10 min to facilitate cell lysis.

GPCR Activity Assay

cAMP formation in iCell Cardiomyocytes was assessed using the CatchPoint cAMP Fluorescent Assay Kit from Molecular Devices, LLC (Table 1). Twenty microliters of iCell cardiomyocyte lysates and a series of 20 μL samples of cAMP standards ($n \geq 6$ wells per standard) covering a concentration range of 0 to 3,300 nM were transferred to a 384-well plate containing goat anti-rabbit IgG-coated wells. Subsequently, 20 μL of a rabbit anti-cAMP antibody solution was added to all wells, except for those that were used for fluorescence background evaluation. In these wells, 20 μL of cAMP assay buffer was added instead. Following gentle shaking for 5 min, 20 μL of horseradish peroxidase-cAMP conjugate was added per well and samples were incubated for 2 h at room temperature. Then, wells were washed four times with 80 μL wash buffer before 50 μL stoplight red substrate solution was added. After 30 min of incubation at room temperature in the dark, fluorescence intensity at 590 nm following excitation at 530 nm was recorded in all wells using the FLIPR tetra instrument (Molecular Devices). cAMP concentrations in cell lysates were then determined using a cAMP standard curve. The sigmoidal curve was fitted to a four-parameter nonlinear regression model using the following equation: $y = (A - D) / (1 + [x/C]^b)$, where x and y are log values of cAMP concentrations and relative fluorescence intensities at 590 nm, respectively. Moreover, in this equation, A and D represent the minimum and maximum asymptotes, B the Hill slope, and C the inflection point (EC_{50}). Curve fitting and data processing were achieved in Prism 5.0 (Graphpad Software, La Jolla, CA).

($1 + [x/C]^b$), where x and y are log values of cAMP concentrations and relative fluorescence intensities at 590 nm, respectively. Moreover, in this equation, A and D represent the minimum and maximum asymptotes, B the Hill slope, and C the inflection point (EC_{50}). Curve fitting and data processing were achieved in Prism 5.0 (Graphpad Software, La Jolla, CA).

High-Content Cell Imaging

For determination of ROS formation, cytotoxicity, and mitochondrial integrity, iPSC cardiomyocytes (50 μL total volume per well) and hepatocytes (25 μL total volume per well) were treated with test chemicals for 30, 60 min, 12, and 24 h (Table 2). Following treatments, 2 \times concentrated staining solution (maintenance medium containing 4 $\mu\text{g}/\text{mL}$ Hoechst 33342, 0.4 μM MitoTracker Orange, and 10 μM CellROX Deep Red) was added and cells were incubated for an additional 30 min at 37°C. Then, cells were washed in the medium before they were fixed for 15 min in 25 μL of 3.7% formaldehyde solution. Cells were then washed thrice with PBS (final volume 25 μL). Cell imaging was then conducted using the ImageX-Press Micro XL system (Molecular Devices). Image acquisition for Hoechst nuclear stain was achieved using the DAPI filter, and MitoTracker and CellROX probes were detected using the Cy3 and C5 filters, respectively. For determination of cytoskeletal integrity and lipid accumulation (Table 3), iPSC hepatocytes were treated with test chemicals for 48 h before they were fixed for 15 min in 25 μL 3.7% formaldehyde. Cells were then washed with PBS and treated for 1 hour with 25 μL 0.02% saponin and 2% fetal bovine serum in PBS. Next, cells were incubated for 2 h at room temperature in 25 μL 165 nM Alexa Fluor[®] 488 Phalloidin solution, followed by 20 min of staining with 25 μL of 4 $\mu\text{g}/\text{mL}$ Hoechst 33342. Cells were then washed twice in PBS before 25 μL LipidTOX Deep Red reagent (1,000 \times diluted in PBS) was added to each well. Approximately 1 h following addition of the LipidTOX reagent, images were acquired using the DAPI (Hoechst 33342), FITC (Alexa Fluor 488 Phalloidin), and Cy5 (LipidTOX) filters. Images were processed and quantified using the multiwavelength cell scoring application module in MetaXpress software (Molecular Devices).

Assay Quality Controls

To evaluate the quality of an assay and the applicability of a particular test chemical to serve as a control substance in an HCS, we either determined the coefficient of variation (% CV) or a Z' -factor analysis, where appropriate. In this study, vehicle (1% v/v DMSO in media)-treated cells served as negative controls, whereas compound-treated cells were treated as positive controls. The % CV value is defined as the standard

Table 2. High-Content Imaging Analysis of Cytotoxicity, Mitochondrial Integrity, and Reactive Oxygen Species Formation in iPSC Cardiomyocytes and iPSC Hepatocytes

Step	Parameter	Value	Description
1	Dispense gelatin solution	25 μ L	0.1% Gelatin in water
2	Incubation time	2 h	37°C
3	Plate cells	25 μ L	5.0 \times 10 ³ (iCell cardiomyocytes)
			1.8 \times 10 ⁴ (iCell hepatocytes 2.0)
4	Incubation time	12 days (iCell cardiomyocytes)	37°C, 5% CO ₂
		8 days (iCell hepatocytes 2.0)	
5	Change media	25/40 μ L (iCell cardiomyocytes)	Every other day (iCell cardiomyocytes)
		25/20 μ L (iCell hepatocytes 2.0)	Every day or every other day (iCell hepatocytes 2.0)
6	Library compounds	10 μ L (iCell cardiomyocytes)	5 \times Conc. stock
		5 μ L (iCell hepatocytes 2.0)	
7	Incubation time	0.5, 1, 12, and 24 h	37°C, 5% CO ₂
8	Dispense 2 \times staining solution	50 μ L (iCell cardiomyocytes)	4 μ g/mL Hoechst, 400 nM MitoTracker® Orange, 10 μ M CellROX® Deep Red Reagent in PBS
		25 μ L (iCell hepatocytes 2.0)	
9	Incubation time	30 min	37°C
10	Wash	Twice	With PBS
11	Dispense fixation solution	25 μ L	3.7% Formaldehyde in PBS
12	Incubation time	15 min	Room temperature
13	Wash	Three times	With PBS
14	Dispense PBS	25 μ L	
15	Acquire images	20 \times objective	With DAPI, Cy3 and Cy5 filters

Step Notes

1. Plate for iCell cardiomyocytes: black, clear bottom 384-well plate (No. 353962; Corning).
- 1, 2. These steps are for iCell cardiomyocytes.
3. iCell cardiomyocytes: Remove gelatin solution before plating cells.
Plate for iCell cardiomyocytes: Collagen I-coated, black, clear bottom 384-well plate (No. 356667; Corning).
5. iCell cardiomyocytes: For cell maintenance, 25 μ L of medium was exchanged every other day. On the evening before the experiment, old medium was replaced with 40 μ L fresh medium.
iCell hepatocytes 2.0: Plating medium was replaced after the first 4 h and subsequently every day for 4 days. Four days following cell seeding, the plating medium was exchanged with maintenance medium. Maintenance medium was replaced every other day until the day of measurements. On the evening before the experiment, old medium was replaced with 20 μ L fresh medium.
6. Final DMSO concentration on assay plate: 1%.
15. ImageXpress was used for image acquisition. Images were acquired within 2 h.

deviation of the vehicle controls. Z' -factors were calculated for cell viability, mitochondrial integrity, and cytoskeletal integrity assays and they were based on the following formula: Z' -factor = $1 - [(3 \times (\sigma_p + \sigma_n)) / (|\mu_n - \mu_p|)]$. In this equation, μ_p and σ_p and μ_n and σ_n represent the means and standard deviations of positive (p) and negative (n) controls.

Depending on the respective assays, numbers of negative controls ranged between 9 and 28 and numbers of positive controls ranged between 3 and 28. To exclude the possibility of vehicle-mediated effects, wells containing untreated cells in media were included on every microplate and results compared with vehicle-treated ones.

Table 3. High-Content Imaging Analysis of Cytotoxicity/Cytoskeletal or Mitochondrial Integrity/Lipid Accumulation in iPSC Hepatocytes

Step	Parameter	Value	Description
1	Plate cells	25 μ L	1.8×10^4 iCell hepatocytes 2.0
2	Incubation time	8 days	37°C, 5% CO ₂
3	Change media	25/20 μ L	Every day or every other day
4	Library compounds	5 μ L	5 \times Conc. stock
5	Incubation time	48 h	37°C, 5% CO ₂
6	Dispense 2 \times staining solution	25 μ L	4 μ g/mL Hoechst, 400 nM MitoTracker Orange in PBS (mitochondria/lipid staining)
7	Wash	Twice	With PBS
8	Dispense fixation solution	25 μ L	3.7% Formaldehyde in PBS
9	Incubation time	15 min	Room temperature
10	Wash	Three times	With PBS
11	Dispense permeabilization solution	25 μ L	0.02% Saponin plus 2% FBS in PBS (cytotoxicity/cytoskeleton staining)
12	Incubation time	10 min	Room temperature 10 min: mitochondria/lipid staining 1 h: cytotoxicity/cytoskeleton staining
		1 h	
13	Dispense actin staining solution	25 μ L	5 units/mL Alexa Fluor [®] 488 Phalloidin at in PBS (cytotoxicity/cytoskeleton staining)
14	Incubation time	2 h	Room temperature (cytotoxicity/cytoskeleton staining)
15	Wash	Three times	With PBS (cytotoxicity/cytoskeleton staining)
16	Dispense nuclei staining solution	25 μ L	2 μ g/mL Hoechst in PBS (cytotoxicity/cytoskeleton staining)
17	Incubation time	20 min	Room temperature (cytotoxicity/cytoskeleton staining)
18	Wash	Three times	With PBS
19.1	Dispense PBS	25 μ L	
19.2	Dispense neutral lipid staining solution	25 μ L	1 \times HCS LipidTOX [®] Deep Red neutral lipid stain in PBS (mitochondria/lipid staining)
20	Acquire images	20 \times objective	With DAPI, Cy3 and Cy5 filters

Step Notes

1. Plate: Collagen I-coated, black, clear bottom 384-well plate (No. 356667; Corning).
3. Plating medium was replaced after the first 4 h and subsequently every day for 4 days. Four days following cell seeding, the plating medium was exchanged with maintenance medium. Maintenance medium was replaced every other day until the day of measurements. On the evening before the experiment, old medium was replaced with 20 μ L fresh medium.
4. Final DMSO concentration on assay plate: 1%
- 6, 19.2. These steps are for mitochondria and lipid staining.
- 11, 13–17, 19.1. These steps are for cytotoxicity and cytoskeletal staining.
20. ImageXpress was used for image acquisition.

HCS, high-content screening.

Curve Fitting and Determination of Point-of-Departure Concentrations

Concentration–response data, excluding those determined for cAMP formation, were initially normalized to vehicle (1% DMSO) controls. To evaluate the concentration–response re-

lationship in individual experiments, normalized data for each chemical and endpoint were used to fit a concentration–response quantitative logistic function as detailed elsewhere.¹³ Point-of-departure (POD) values were defined as the concentrations at which the concentration–response curve

increases or decreases more than one standard deviation of the vehicle controls.

RESULTS

Combined Calcium Flux and GPCR Activity Measurements in iPSC Cardiomyocytes

Effects of test chemicals on cardiomyocyte beating frequency were determined by intracellular calcium flux measurements using the FLIPR tetra instrument. Reference chemicals in-

cluded a positive chronotrope (isoproterenol), a negative chronotrope (propranolol), two potassium channel blockers (cisapride and sotalol), and three cytotoxic agents (TAB, menadione, and doxorubicin). Calcium flux measurements in untreated (cell medium added) and vehicle-treated cardiomyocytes indicated a decrease in the beat frequency 10 min and 30 min following cellular manipulation (*i.e.*, addition of chemicals or vehicle into wells); the beating frequency had recovered to basal levels after one hour (*Fig. 2A*). There were

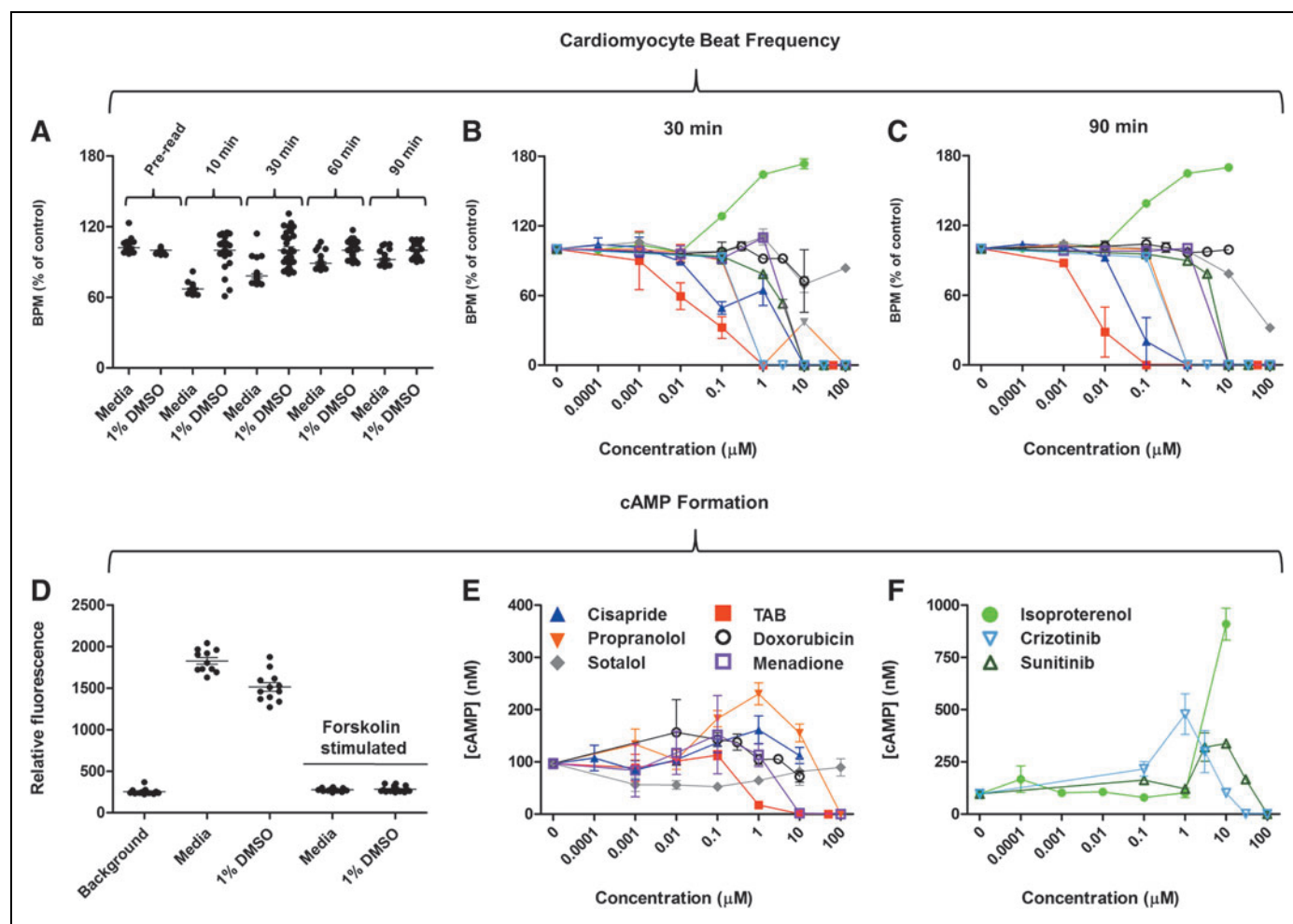


Fig. 2. Assessment of cardiophysiological effects of isoproterenol (green circle), TAB (red square), cisapride (blue triangle), propranolol (orange triangle), sotalol (gray diamond), doxorubicin (open black circle), menadione (open purple square), sunitinib (open green triangle), crizotinib (open blue triangle) by combined calcium flux monitoring, and cAMP formation. **(A)** Basal cardiomyocyte beat frequencies after 0 (pre-read), 10, 30, 60, and 90 min following addition of 1:5 (v/v) medium or vehicle (1% DMSO in medium). **(B, C)** Concentration-response plots showing effects of drugs on cardiomyocyte beat frequencies after 30 and 90 min. The potential for GPCR activation was assessed by measuring intracellular cAMP levels by competitive ELISA. **(D)** Evaluation of GPCR assay controls: background fluorescence at 590 nm was determined using cAMP-free assay buffer and omitting Rabbit anti-cAMP antibody. Treatment with cell medium and vehicle was used to determine basal cAMP levels in cardiomyocytes; stimulation of cells with 20 μ M forskolin was used as a positive control, resulting in maximum cAMP formation and competitive repression of the cAMP-horseradish peroxidase signal. **(E)** Concentration-response plots of drugs that did not, or only slightly, affect GPCR activity in cardiomyocytes. **(F)** Concentration-response plots of three drugs that significantly (twofold or more) increased cAMP formation in cardiomyocytes. Data points in all plots represent mean \pm SEM of at least three replicates. DMSO, dimethyl sulfoxide; TAB, tetrabutylammonium bromide.

no significant differences in untreated and vehicle-treated cells after 60 and 90 min, and the baseline cell function parameters being recorded in this study were similar to those reported previously.^{12,13} The % CV for calcium flux measurements 90 min following exposure to test chemicals was determined as 6%, and consequently the assay was capable of detecting a deviation of 18% from the mean of vehicle-treated cells (Table 4).

As early as 30 min following initial exposure to test chemicals, expected phenotypic responses could be observed for all reference compounds. However, after 60 min, the concentration–response profiles were much clearer and provided a reliable readout until at least 90 min, with isoproterenol being the only drug to induce a concentration-dependent increase in the cardiac beat frequency (Fig. 2B, C). Increases in cardiomyocyte beating frequency (beats per minute) at concentrations higher than 0.1 μM were all statistically significant ($P < 0.001$), just as decreases in cardiomyocyte beat rates observed for TAB ($\geq 0.01 \mu\text{M}$), cisapride ($\geq 0.1 \mu\text{M}$), crizotinib and propranolol ($\geq 1 \mu\text{M}$), and menadione, sunitinib, and sotalol ($\geq 10 \mu\text{M}$). In addition, it should be noted that isoproterenol, cisapride, and sotalol were all excellent qualitative reference compounds for their respective phenotypes (data not shown). Propranolol was found to be an acceptable control; however, its negative chronotropic effects were most stable at the earlier time points (10–30 min).

After 90 min of calcium flux measurements, cells were used in a competitive ELISA to determine intracellular cAMP levels.

Increases in cAMP formation are an indicator of GPCR activation, a mechanism by which cardiotoxic chemicals can induce chronotropic effects. cAMP formation in positive controls was stimulated with 20 μM forskolin and resulted in suppression of the fluorescence signal to background levels (Fig. 2D). The % CV, based on variability of cAMP concentrations in vehicle-treated cardiomyocytes, was 12% and therefore increases in cAMP formation of 36% or more are detectable in this assay (Table 4). Most of the reference chemicals did not, or only marginally, affect intracellular cAMP levels (Fig. 2E); however, crizotinib, sunitinib, and isoproterenol increased cAMP levels three to ninefold (Fig. 2F).

High-Content Imaging of iPSC Cardiomyocytes

Cytotoxicity, mitochondrial integrity, and ROS formation in iPSC cardiomyocytes were comprehensively assessed by high-content imaging after 30 min, 1, 12, and 24 h (Fig. 3). Vehicle controls for all three probes did not differ from untreated cells across all time points (Fig. 3, left column). Concentration–effect profiles for cell viability and mitochondrial integrity correlated well for TAB, doxorubicin, menadione, and crizotinib at all time points. Z' -factor analysis provided supporting evidence for the utility of TAB, menadione, and crizotinib for HCS applications of cell viability and mitochondrial integrity, yielding Z' -factors ranging between 0.7 and 0.8 (Table 4). By contrast, ROS formation was best observed after just 30 min in cells treated

Table 4. Assay Quality Control–iCell Cardiomyocytes

Assay	Description	Time	Control	%CV ^a	Z' -factor ^b
Calcium flux	Cardiomyocyte beating assay	90 min	1% DMSO in media	6%	
cAMP formation	GPCR activation	90 min	1% DMSO in media	12%	
ROS formation	Cytotoxicity measurement	30 min	1% DMSO in media	1%	
Cell viability	Cytotoxicity measurement	30 min, 24 h	TAB (50 μM)		0.8, 0.7
			Menadione (100 μM)		0.8 (24 h)
			Crizotinib (100 μM)		0.8, 0.8
Mitochondrial integrity	Cytotoxicity measurement	30 min, 24 h	TAB (50 μM)		0.8, 0.8
			Menadione (100 μM)		0.8 (24 h)
			Crizotinib (100 μM)		0.8, 0.8

^aStandard deviation expressed as percentage of the mean of vehicle-treated controls, calculated from 28 calcium flux, 12 cAMP formation, and 9 ROS formation replicates, respectively.

^bCalculated from 9 negative and 3 positive control replicates. Z' values separated by a comma represent determinations following cell viability measurements after 30 min and 24 h, respectively. In the case of menadione, a Z' -factor was determined after 24 h only. CV, coefficient of variation; ROS, reactive oxygen species; TAB, tetraoctylammonium bromide.

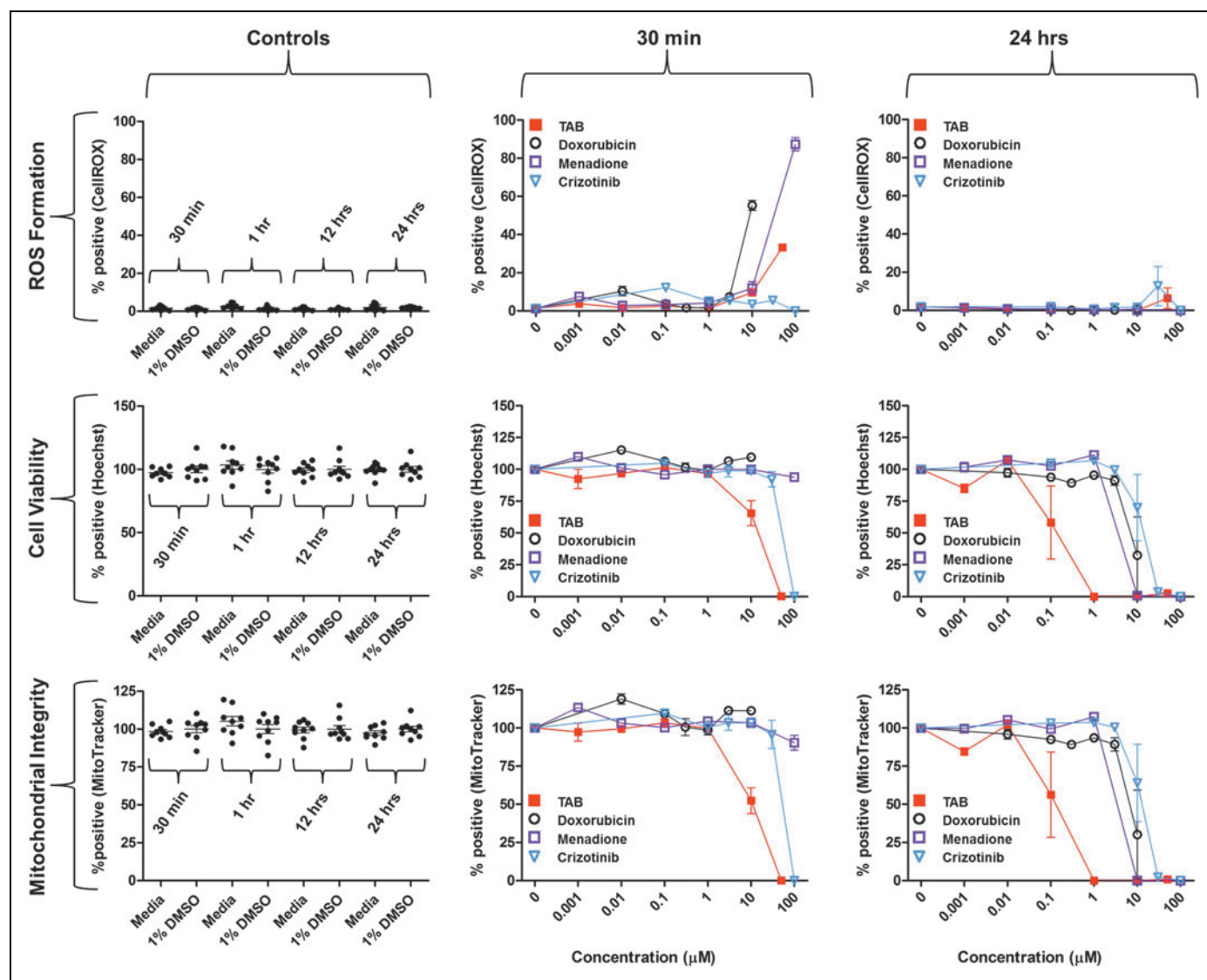


Fig. 3. Combined assessment of ROS formation, cytotoxicity, and mitochondrial integrity in iPSC cardiomyocytes. The *upper row* summarizes results on ROS formation, the *second and third rows* depict data derived from nuclear and mitochondrial imaging for evaluation of cytotoxicity and mitochondrial integrity. The *left column* includes plots showing basal levels (percentages of cells with elevated levels of ROS, viable cells, and cells with intact mitochondria) of medium and vehicle (1% DMSO in medium)-treated cardiomyocytes. The *second and third columns* show concentration-response plots for TAB (red square), doxorubicin (open black circle), menadione (open purple square), and crizotinib (open blue triangle) after 30 min and 24 h of incubation. All data points represent mean \pm SEM.

with 50 μ M TAB, 10 μ M doxorubicin, and 100 μ M menadione, and these effects were significantly abrogated after 24 h (Fig. 3, first row, and Supplementary Fig. S1; Supplementary Data are available online at www.liebertpub.com/adt). Doxorubicin and menadione provide excellent reference standards for ROS detection in HCS applications after 30 min, significantly ($P < 0.001$) exceeding the minimum detectable increases in ROS-positive cells of 3%, based on a determined % CV of 1%.

Combined Assessment of Cell Viability and Cytoskeletal Integrity and Mitochondrial Integrity and Lipid Accumulation in iPSC Hepatocytes

The feasibility of combining nuclear and actin stains, as well as mitochondrial and lipid accumulation probes, for high-content imaging of iPSC hepatocytes was evaluated by incubating cells for 48 h in the presence of TAB, aflatoxin B1, amiodarone, menadione, sunitinib, and crizotinib. In vehicle-treated cells, no effects on these parameters were observed

compared with untreated cells (Fig. 4, top row) and the baseline cell function parameters being recorded in this study were similar to those reported previously.¹⁴ Concentration-effect profiles correlated well for all reference compounds for cell viability, cytoskeletal integrity, and mitochondrial integrity (Fig. 4, bottom row and *Supplementary Fig. S2A*). Moreover, we observed concentration-dependent increases in lipid accumulation in hepatocytes after treatment with TAB, amiodarone, crizotinib, and sunitinib. The assay is capable of reliably detecting an increase in neutral lipid accumulation of 7.5% based on a % CV of 2.5%. Amiodarone, a known steatosis inducer, was identified in this study as the most effective reference chemical and produced significant ($P < 0.001$) lipid accumulation in about 84% of hepatocytes at concentrations ranging between 30 and 100 μM (*Supplementary Fig. S2B*). Crizotinib and sunitinib yielded positive results ($\sim 60\%$ positive cells at 30 μM concentrations) as well. All three compounds were also very efficient in disrupting cytoskeletal integrity ($Z' = 0.9\text{--}1.0$) of iPSC hepatocytes.

Simultaneous Assessment of Cytotoxicity, Mitochondrial Integrity, and ROS Formation in iPSC Hepatocytes

Following exposure to TAB, doxorubicin, menadione, crizotinib, and sunitinib for 30 min, 1, 12, and 24 h, cells were stained with Hoechst 33342, MitoTracker Orange, and Cell-

ROX Deep Red fluorescence probes to determine effects on cell viability, mitochondrial integrity, and the potential for ROS formation (Fig. 5 and *Supplementary Fig. S3*). In vehicle-treated cells, no effects on these parameters were observed compared with untreated cells (Fig. 5, left column). There was a strong correlation between concentration-response profiles for cell viability and mitochondrial integrity for all chemicals at all time points (Fig. 5, middle and bottom rows). However, there were only limited cytotoxic effects observed after 30 min of exposure, whereas cytotoxicity was more pronounced after 24 h.

ROS formation was only observed after 30 min in cells treated with 100 μM menadione, yielding 61% positive cells ($P < 0.001$). Whereas comparable with results obtained for iPSC cardiomyocytes, ROS formation was undetectable after 24 h (Fig. 3, first row). The % CV of vehicle-treated hepatocytes after 30 min was 1% and thus also correlated well with the value determined for cardiomyocytes (Table 5). By contrast, there were few cytotoxic effects observable at early time points. Only in cells treated with TAB and crizotinib, loss of cell viability and mitochondrial integrity was evident after 30 min. However, all five chemicals were identified as good standards for cell viability detection 24 h after treatment, with Z' -factors ranging between 0.6 (10 μM menadione) and 0.7 (all other test compounds). For mitochondrial integrity studies,

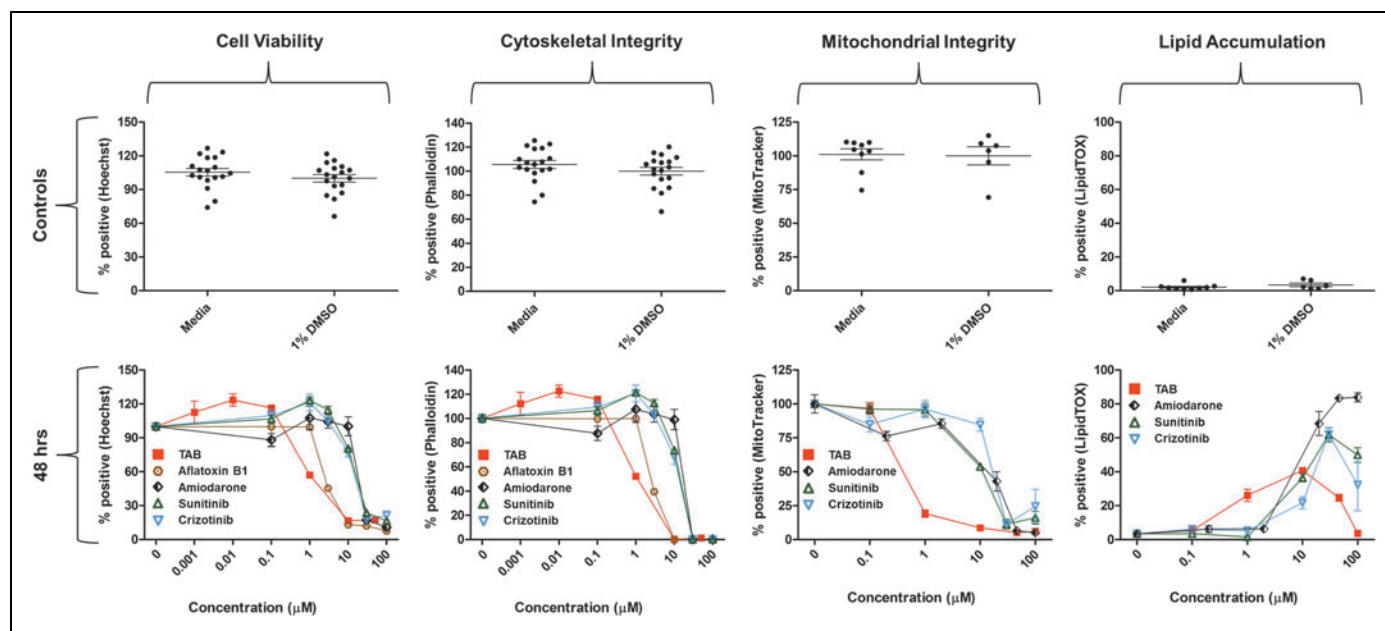


Fig. 4. Combined assessment of cytotoxicity (column 1), cytoskeletal integrity (column 2), mitochondrial integrity (column 3), and lipid accumulation (column 4) in iPSC hepatocytes. Upper row: Basal percentages of control cells with intact nuclei, cytoskeletal integrity, mitochondria, and lipid accumulation 48 h following treatment with medium and vehicle (1% DMSO in medium). Lower row: Concentration-response plots of hepatocytes treated with TAB (red square), aflatoxin B1 (brown hexagon), amiodarone (black and white diamond), menadione (open purple square), crizotinib (open blue triangle), and sunitinib (open green triangle) for 48 h. Data points represent mean \pm SEM.

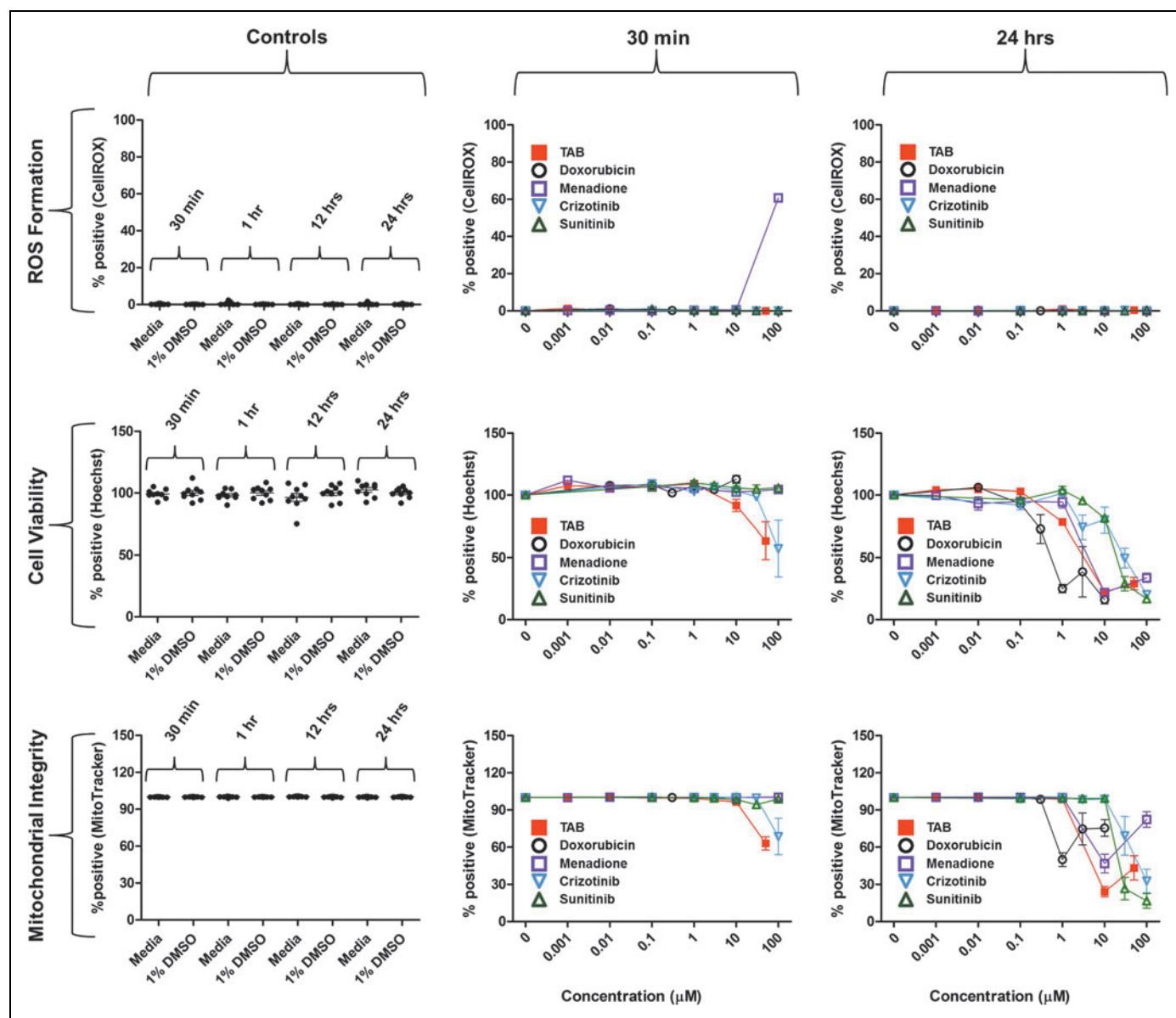


Fig. 5. Combined assessment of ROS formation, cytotoxicity, and mitochondrial integrity in iPSC hepatocytes. The *first row* summarizes results on ROS formation, the *second and third rows* depict data derived from nuclear and mitochondrial imaging for evaluation of cytotoxicity and mitochondrial integrity. The *left column* includes plots summarizing basal levels (percentages of cells with elevated levels of ROS, viable cells, and cells with intact mitochondria) of medium and vehicle (1% DMSO in medium)-treated cardiomyocytes. The *second and third columns* show concentration–response plots for TAB (red square), doxorubicin (open black circle), menadione (open purple square), and crizotinib (open blue triangle) after 30 min and 24 h of incubation. All data points represent mean \pm SEM. Combined assessment of ROS formation, cytotoxicity, and mitochondrial integrity in iPSC hepatocytes treated with TAB (red square), doxorubicin (open black circle), menadione (open purple square), crizotinib (open blue triangle), and sunitinib (open green triangle) for up to 24 h. Plots show comparisons between untreated and vehicle (1% DMSO)-treated cells and high-content imaging-derived concentration–response profiles. Data points represent mean \pm SEM.

sunitinib had the highest Z' -factor ($Z' = 0.6$). TAB and crizotinib were also reasonable (Z' -factors of 0.1 and 0.3, respectively) controls, but doxorubicin and menadione yielded considerable variability and they should not be used as reference compounds in these HCS applications.

Determination of POD Benchmark Concentrations

While the effective concentration at 50% of the maximum assay response (EC_{50}) remains one of the most frequently utilized parameters for comparison of concentration–response data in biochemical assays, it requires a clearly

Table 5. Assay Quality Control—iCell Hepatocytes

Assay	Description	t	Control	%CV ^a	Z'-Factor ^b
ROS formation	Cytotoxicity measurement	30 min	1% DMSO in media	1%	
Cell viability	Cytotoxicity measurement	24 h	TAB (50 μM)		0.7
			Doxorubicin (10 μM)		0.7
			Menadione (10 μM)		0.6
			Crizotinib (100 μM)		0.7
			Sunitinib (100 μM)		0.7
Mitochondrial integrity	Cytotoxicity measurement	24 h	TAB (50 μM)		0.1
			Doxorubicin (10 μM)		-0.5
			Menadione (100 μM)		-0.9
			Crizotinib (100 μM)		0.3
			Sunitinib (100 μM)		0.6
Cytoskeletal integrity	Cytotoxic agents/cytoskeletal poisons	48 h	TAB (50 μM)		0.7
			Aflatoxin B1 (100 μM)		1.0
			Amiodarone (100 μM)		0.9
			Crizotinib (100 μM)		1.0
			Sunitinib (100 μM)		1.0
Lipid accumulation	Steatosis inducer	48 h	1% DMSO in media	2.5%	

^aStandard deviation expressed as percentage of the mean of vehicle-treated controls, calculated from nine ROS formation or six lipid accumulation replicates, respectively.

^bCalculated from 3 positive control replicates and 9 cell viability, 9 mitochondrial integrity, or 18 cytoskeletal integrity negative controls, respectively.

defined maximum effect level. However, a maximum assay response is not always clearly defined (*e.g.*, cAMP formation assay), thereby limiting the overall applicability of the EC₅₀ for the evaluation of HCS data. As a toxicologically relevant and more broadly applicable alternative, we have determined POD concentrations as reference values for test chemicals in this study (Table 6). As recommended by the US Environmental Protection Agency for quantitative assessment of toxicity data, we applied a derivation of one standard deviation of vehicle-treated control wells to define the POD value.²⁴ In cases where its effect did not deviate from the mean control by more than one standard deviation, the compound was deemed nontoxic under these assay conditions and the POD was considered inapplicable. Determined POD values were generally consistent with the curve fitting and reflected increased cytotoxic effects observed after 24 and 48 h compared

with early time points (30 min) (*i.e.*, POD values for cytotoxic parameters generally decreased over time).

Application of Combinatorial HCS Assays for Toxicity Profiling of Complex Substances

To test the applicability of combinatorial HCS assays for toxicological characterization of chemically complex substances, we determined cardiophysiological effects of two DMSO extracts of commercial gas oils. We used a combination of the calcium flux and GPCR activity assays as described above. Both extracts exhibited highly similar concentration-effect profiles (Fig. 6). At concentrations less than 10 ng/L, concentration-dependent increases in cardiomyocyte beat frequency were observed, whereas there was a sharp decline in cardiomyocyte function and viability at concentrations exceeding 10 ng/L. In both instances, positive chronotropic effects correlated well with intracellular cAMP levels, indicating

Table 6. POD Concentrations

Assay	Reference chemical	iCell cardiomyocytes (μM)			iCell hepatocytes (μM)		
		30 min	90 min	24 h	30 min	24 h	48 h
Calcium flux	Isoproterenol	–	0.01	–	–	–	–
	Sotalol	–	2.7	–	–	–	–
	Cisapride	–	0.01	–	–	–	–
	Propranolol	–	0.14	–	–	–	–
	TAB ^b	–	0.0006	–	–	–	–
	Menadione	–	2.4	–	–	–	–
	Sunitinib	–	2.3	–	–	–	–
	Crizotinib	–	0.18	–	–	–	–
cAMP formation	Isoproterenol	–	2.4	–	–	–	–
	Crizotinib	–	0.02	–	–	–	–
	Sunitinib	–	3	–	–	–	–
Cell viability	TAB	6	–	0.05	8.7	0.8	0.7
	Doxorubicin	Nontoxic	–	2.18	Nontoxic	0.1	–
	Menadione	Nontoxic	–	3.7	Nontoxic	0.9	–
	Crizotinib	30	–	6.3	40.3	0.4	9.1
	Aflatoxin B1	–	–	–	–	–	1.8
	Amiodarone	–	–	–	–	–	16.2
	Sunitinib	–	–	–	Nontoxic	5	9.2
Mitochondrial integrity	TAB	3.8	–	0.04	3.1	0.8	0.2
	Doxorubicin	Nontoxic	–	1.58	Nontoxic	0.2	–
	Menadione	84	–	3.1	Nontoxic	0.6	–
	Crizotinib	30	–	5.8	27.5	4.8	10.1
	Amiodarone	–	–	–	–	–	11.7
	Sunitinib	–	–	–	Nontoxic	8	7.8
ROS formation	TAB	2.6	–	–	–	–	–
	Doxorubicin	1.8	–	–	–	–	–
	Menadione	1.2	–	–	5.5	–	–
Cytoskeletal integrity	TAB	–	–	–	–	–	0.7
	Crizotinib	–	–	–	–	–	9.2
	Aflatoxin B1	–	–	–	–	–	1.9
	Amiodarone	–	–	–	–	–	13.5
	Sunitinib	–	–	–	–	–	8.3

(continued)

Table 6. (Continued)

Assay	Reference chemical	iCell cardiomyocytes (μM)			iCell hepatocytes (μM)		
		30 min	90 min	24 h	30 min	24 h	48 h
Lipid accumulation	TAB	–	–	–	–	–	0.1
	Crizotinib	–	–	–	–	–	6.4
	Amiodarone	–	–	–	–	–	6.4
	Sunitinib	–	–	–	–	–	6.6

Value at which the concentration–response curve deviates from the mean control by more than one standard deviation. POD values are derived from a single curve fit using three individual replicate data points per concentration.

POD, point-of-departure.

that GPCR activation is a mechanism for gas oil extract-induced contractility.

DISCUSSION

The development of novel HCS approaches that combine the application of physiologically relevant *in vitro* models with multiparametric biological phenotyping is among the most promising innovations in toxicological research and pharmaceutical drug development.^{1,2,10} The broad applicability of HCS to a variety of next-generation assays, including, but not limited to, cell imaging, genomics, metabolomics, and computational modeling, bears vast potential to overcome the limitations of traditional *in vitro* and *in vivo* toxicity testing. In particular, these technologies are promising candidates to close the existing data gaps in safety testing of industrial and environmental chemicals and to lead to the reduction and possibly replacement of animal use in toxicity testing.^{25,26}

In this study, we explored innovations to HCS approaches to enhance the comprehensiveness of toxicity profiling using iPSC cardiomyocytes and hepatocytes. The selection of these cell types was based on a number of considerations. First, cardiotoxicity and hepatotoxicity are among the most prevalent causes for drug attrition in clinical trials, and improvements in preclinical predictive safety testing are highly desirable.^{27,28} Moreover, cardiotoxicity testing typically requires animal models, primarily dogs, which is challenging from both an ethical and an economical perspective.²⁹ Second, iPSC cardiomyocytes and hepatocytes are amenable to HCS applications and are physiologically similar to primary cells, which arguably positions them among the most relevant *in vitro* models available to date.

Kinetic assessment of cardiophysiological effects of reference chemicals was conducted by intracellular calcium flux measurements and combined with a competitive ELISA to determine and correlate cAMP concentrations in treated

cardiomyocytes. Increases in intracellular cAMP are indicative of GPCR activation, including the β -adrenergic receptor, which is a known mechanism of isoproterenol-induced cardiomyocyte stimulation.³⁰ Our results reflect these characteristics and indicate approximately ninefold increases in cAMP levels and almost doubling in the cardiomyocyte beat rate upon treatment with 10 μM isoproterenol, a finding that is consistent with previous observations reported in Sirenko *et al.*¹² Likewise, observed calcium flux patterns (data not shown) and concentration–response curves for cisapride and propranolol were also consistent with results of Sirenko *et al.*¹² Increases in cAMP formation observed following treatment with crizotinib and sunitinib were negatively correlated with cardiomyocyte beat frequency. Determined POD values (0.2 and 2.3 μM) are consistent with previous findings for both drugs.³¹

We also applied this assay combination for the evaluation of cardiophysiological effects of two very chemically complex substances, gas oil extracts. This experiment was intended to test the applicability of combinatorial HCS approaches to chemically undefined, complex, and comparably hydrophobic substances. The hazard assessment of such substances and mixtures represents a current major challenge in the field of safety assessment; novel approaches for characterization of their potential human health hazard are needed. The fact that we used a relatively high concentration of DMSO (1%) as a vehicle during assay development allowed us to treat cells with gas oil extracts in the ng/L range. Importantly, the calcium flux measurements provided a clear indication of a biphasic curve consisting of increases in the beat rate at low concentrations and loss of beating at concentrations exceeding 10 ng/L. A clear correlation between beat frequencies and cAMP levels in cardiomyocytes treated with both gas oil extracts provided mechanistic evidence that GPCR activation is associated with their chronotropic effects. Such similarity is

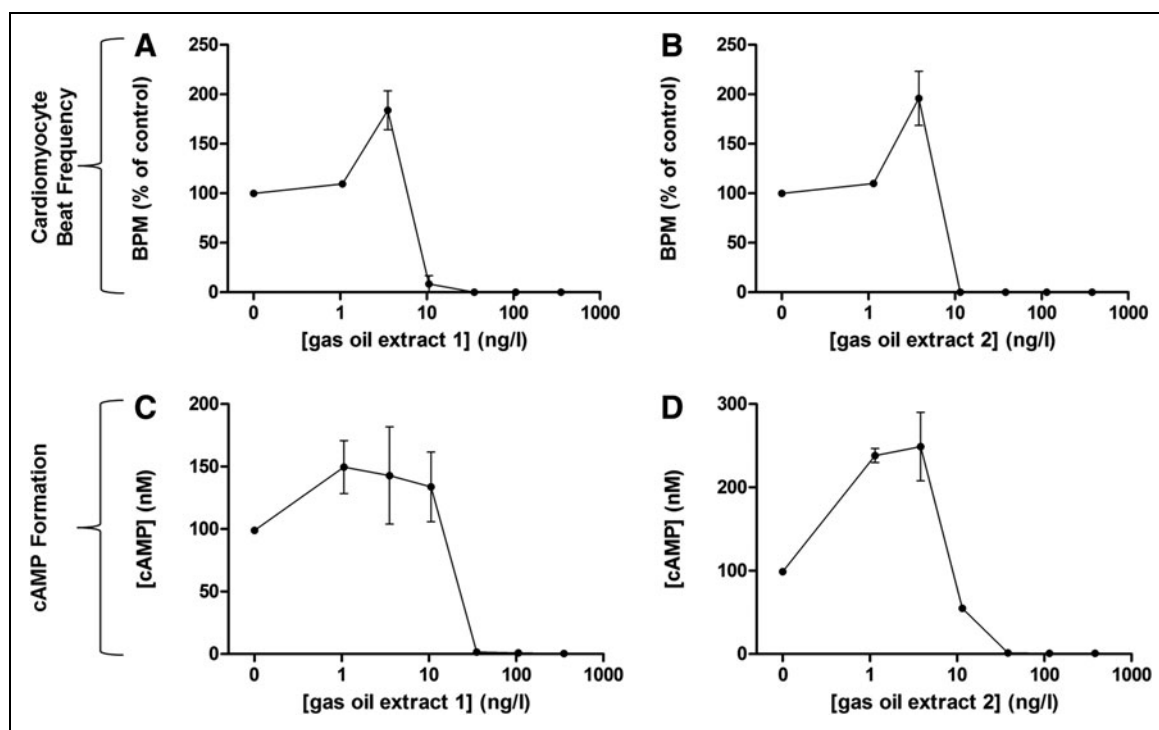


Fig. 6. Application of combinatorial high-content screening assays for descriptive and mechanistic toxicity profiling of complex mixtures. Plots show (A–B) cardiomyocyte beat frequency (beats per minute, BPM) and (C–D) cAMP formation concentration–response profiles for two (A and C; B and D) DMSO extracts of commercial gas oils. Individual data points and mean \pm SEM are indicated for each concentration. Cardiomyocyte beat frequency profiles demonstrate initial chronotropic effects (\leq 1% dilution), followed by total inhibition of cardiomyocyte beating, an indicator of cell death. Moreover, cardiac chronotropic effects correlate well with cAMP formation, a cellular indicator of GPCR stimulation.

promising and shows that the use of multiplexed assays may allow for using the similarity in the toxicological effects as a justification for grouping complex and chemically undefined substances into categories for registration and labeling.³² Consequently, we are hereby providing an example of how combinatorial HCS can be applied to provide both descriptive and mechanistic toxicity data in a time- and resource-saving format.

In addition, we tested the best conditions for high-content imaging to simultaneously evaluate various biological phenotypes for both iPSC cardiomyocytes and hepatocytes. First, we combined nucleic acid, mitochondria, and ROS-specific fluorescent dyes to quantify cell viability, mitochondrial integrity, and ROS formation in chemically treated cells. Our results show that for this type of analysis, at least two time points should be considered. ROS formation was observable after 30 min in both cell types, but ROS staining intensity had decreased to basal levels in almost all instances after 24 h. By contrast, cytotoxicity and loss of mitochondrial integrity, both of which were highly correlated, were more apparent after 24 h than at early time points, particularly in hepatocytes. Our results show that menadione is an excellent choice

for a positive control for ROS formation in HCS of both cell types, with comparable POD values (1.2 μ M in cardiomyocytes; 5.5 μ M in hepatocytes) that are in agreement with previous observations in Caco-2 and HepG2 cells.^{33,34} All reference chemicals were excellent inducers of cell death after 24 h, and we recommend crizotinib and sunitinib as controls for HCS evaluation of the mitochondrial integrity.

In addition to these probes, we applied actin and neutral lipid stains in iPSC hepatocytes to assess cytoskeletal integrity and lipid accumulation 48 h following treatment. Hepatic steatosis is one of the most prevalent, clinically relevant liver toxicities and a common side effect encountered at the clinical trial stage in drug development.³⁵ Concentration–response profiles of TAB, aflatoxin B1, amiodarone, menadione, and crizotinib for cell viability and mitochondrial integrity correlated well with those obtained for cytoskeletal integrity. Viability data, including concentration–response curves, for crizotinib and sunitinib also correlated well with previously published results.³¹ Effects of aflatoxin B1 on cytoskeletal integrity had previously revealed the chemical as a highly promising reference chemical in HCS applications.¹⁴ However, besides aflatoxin B1, amiodarone, crizotinib, and

sunitinib also provided excellent references to detect the loss of cytoskeletal integrity. Lipid accumulation in iPSC hepatocytes was negatively correlated with mitochondrial integrity and there was a concentration-dependent increase in the lipid staining intensity for all probes. However, amiodarone, a prominent steatosis inducer, was the most efficient drug in this assay, increasing the number of cells with detectable lipid accumulation to above 80% at concentrations exceeding 10 μM .^{22,35} In fact, the concentration–response curve for amiodarone and the determined POD of 6.4 μM are concordant with previous reports on neutral lipid and triglyceride accumulation in iPSC hepatocytes and HepaRG cells.^{14,36}

Altogether, this study provides a novel strategy toward rapid and cost-efficient multiparametric HCS for quantitative *in vitro* profiling of cardiotoxicity and hepatotoxicity that is not only amenable to drug screening but also for the assessment of the potential hazard of highly complex and relatively hydrophobic substances (e.g., petroleum substances). Importantly, by combining various assays, it is possible to derive mechanistic toxicity data that complement descriptive toxicity assessments while also achieving replacement of animal testing. Even though this work focused primarily on the application of high-content imaging techniques, and there are a number of inherent limitations to HCS or any other type of *in vitro* toxicity screening, the potential for combining HCS with additional emerging technologies such as quantitative genomics and metabolomics should be addressed in future studies.

ACKNOWLEDGMENTS

The authors appreciate excellent technical assistance from Ms. Arlean Rohde (Concawe, Brussels, Belgium) and Dr. Tim Roy (University of South Carolina–Beaufort), who coordinated preparation of gas oil extracts. In addition, the authors would like to thank Dr. Fred Wright and Dr. Yi-Hui Zhou (North Carolina State University) for providing the custom R script that was used to calculate the POD benchmark concentrations. The funding for this work was provided, in part, by grants from the U.S. Environmental Protection Agency (STAR RD83516601 and RD83574701). F. Grimm was a recipient of the Society of Toxicology–Colgate Palmolive Postdoctoral Fellowship in *in vitro* toxicology. O. Sirenko was employed by Molecular Devices, LLC (Sunnyvale, CA), the manufacturer of several instruments used in this work: FLIPR tetra and ImageXpress Micro XS.

DISCLOSURE STATEMENT

O.S. was employed by Molecular Devices, LLC (Sunnyvale, CA), the manufacturer of several instruments used in this work: FLIPR tetra and ImageXpress Micro XS.

REFERENCES

- McPartland J, Dantzker HC, Portier CJ: Building a robust 21st century chemical testing program at the U.S. Environmental Protection Agency: recommendations for strengthening scientific engagement. *Environ Health Perspect* 2015;123:1–5.
- Settivari RS, Ball N, Murphy L, Rasoulpour R, Boverhof DR, Carney EW: Predicting the future: opportunities and challenges for the chemical industry to apply 21st-century toxicity testing. *J Am Assoc Lab Anim Sci* 2015;54:214–223.
- Landrigan PJ, Goldman LR: Chemical safety, health care costs and the Affordable Care Act. *Am J Ind Med* 2014;57:1–3.
- Adeleye Y, Andersen M, Clewell R, et al.: Implementing Toxicity Testing in the 21st Century (TT21C): Making safety decisions using toxicity pathways, and progress in a prototype risk assessment. *Toxicology* 2014;332:102–111.
- Dix DJ, Houck KA, Martin MT, Richard AM, Setzer RW, Kavlock RJ: The ToxCast program for prioritizing toxicity testing of environmental chemicals. *Toxicol Sci* 2007;95:5–12.
- Tice RR, Austin CP, Kavlock RJ, Bucher JR: Improving the human hazard characterization of chemicals: a Tox21 update. *Environ Health Perspect* 2013; 121:756–765.
- Xia M, Huang R, Witt KL, et al.: Compound cytotoxicity profiling using quantitative high-throughput screening. *Environ Health Perspect* 2008;116: 284–291.
- Sundberg SA: High-throughput and ultra-high-throughput screening: solution- and cell-based approaches. *Curr Opin Biotechnol* 2000;11:47–53.
- An WF, Tolliday N: Cell-based assays for high-throughput screening. *Mol Biotechnol* 2010;45:180–186.
- Jennings P: The future of *in vitro* toxicology. *Toxicol In Vitro* 2014;1217–1221.
- Singh VK, Kalsan M, Kumar N, Saini A, Chandra R: Induced pluripotent stem cells: applications in regenerative medicine, disease modeling, and drug discovery. *Front Cell Dev Biol* 2015;3:1–18.
- Sirenko O, Crittenden C, Callamaras N, et al.: Multiparameter *in vitro* assessment of compound effects on cardiomyocyte physiology using iPSC cells. *J Biomol Screen* 2013;18:39–53.
- Sirenko O, Cromwell EF, Crittenden C, Wignall JA, Wright FA, Rusyn I: Assessment of beating parameters in human induced pluripotent stem cells enables quantitative *in vitro* screening for cardiotoxicity. *Toxicol Appl Pharmacol* 2013;273:500–507.
- Sirenko O, Hesley J, Rusyn I, Cromwell EF: High-content assays for hepatotoxicity using induced pluripotent stem cell-derived cells. *Assay Drug Dev Technol* 2014;12:43–54.
- Ma J, Guo L, Fiene SJ, et al.: High purity human-induced pluripotent stem cell-derived cardiomyocytes: electrophysiological properties of action potentials and ionic currents. *Am J Physiol Heart Circ Physiol* 2011;301:H2006–H2017.
- Guguen-Guillouzo C, Corlu A, Guillouzo A: Stem cell-derived hepatocytes and their use in toxicology. *Toxicology* 2010;270:3–9.
- Hahn VS, Lenihan DJ, Ky B: Cancer therapy-induced cardiotoxicity: basic mechanisms and potential cardioprotective therapies. *J Am Heart Assoc* 2014; 3:e000665.
- Njoku DB: Drug-induced hepatotoxicity: metabolic, genetic and immunological basis. *Int J Mol Sci* 2014;15:6990–7003.
- Sturgill MG, Lambert GH: Xenobiotic-induced hepatotoxicity: mechanisms of liver injury and methods of monitoring hepatic function. *Clin Chem* 1997;43:1512–1526.
- Russmann S, Kullak-Ublick GA, Grattagliano I: Current concepts of mechanisms in drug-induced hepatotoxicity. *Curr Med Chem* 2009;16: 3041–3053.
- Garside H, Marcoe KF, Chesnut-Speelman J, et al.: Evaluation of the use of imaging parameters for the detection of compound-induced hepatotoxicity in 384-well cultures of HepG2 cells and cryopreserved primary human hepatocytes. *Toxicol In Vitro* 2014;28:171–181.
- Germano D, Uteng M, Pognan F, Chibout SD, Wolf A: Determination of liver specific toxicities in rat hepatocytes by high content imaging during 2-week multiple treatment. *Toxicol In Vitro* 2014;pii:S0887-2333(14)00089-7.

23. ASTM International: Standard Test Method for Determining Carcinogenic Potential of Virgin Base Oils in Metalworking Fluids. In *E1687-10*. ASTM International, West Conshohocken, PA, 2010. Available at www.astm.org/DATABASE.CART/HISTORICAL/E1687-10.htm (last accessed September 25, 2015).
24. U.S. EPA: *Benchmark Dose Technical Guidance*. Risk Assessment Forum, US EPA: Washington, DC, 2012. Available at www2.epa.gov/osa/benchmark-dose-technical-guidance (last accessed September 25, 2015)
25. Gilbert N: Data gaps threaten chemical safety law. *Nature* 2011;475:150–151.
26. Michelini E, Cevenini L, Calabretta MM, Calabria D, Roda A: Exploiting in vitro and in vivo bioluminescence for the implementation of the three Rs principle (replacement, reduction, and refinement) in drug discovery. *Anal Bioanal Chem* 2014;406:5531–5539.
27. Ferri N, Siegl P, Corsini A, Herrmann J, Lerman A, Benghozi R: Drug attrition during pre-clinical and clinical development: understanding and managing drug-induced cardiotoxicity. *Pharmacol Ther* 2013;138:470–484.
28. Roberts RA, Kavanagh SL, Mellor HR, Pollard CE, Robinson S, Platz SJ: Reducing attrition in drug development: smart loading preclinical safety assessment. *Drug Discov Today* 2014;19:341–347.
29. Casartelli A, Lanzoni A, Comelli R, et al.: A novel and integrated approach for the identification and characterization of drug-induced cardiac toxicity in the dog. *Toxicol Pathol* 2011;39:361–371.
30. Li X, Nooh MM, Bahouth SW: Role of AKAP79/150 protein in beta1-adrenergic receptor trafficking and signaling in mammalian cells. *J Biol Chem* 2013;288:33797–33812.
31. Doherty KR, Wappel RL, Talbert DR, et al.: Multi-parameter in vitro toxicity testing of crizotinib, sunitinib, erlotinib, and nilotinib in human cardiomyocytes. *Toxicol Appl Pharmacol* 2013;272:245–255.
32. Berggren E, Amcoff P, Benigni R, et al.: Chemical safety assessment using read-across: assessing the use of novel testing methods to strengthen the evidence base for decision making. *Environ Health Perspect* 2015 [Epub ahead of print] DOI:10.1289/ehp.1409342.
33. Briede JJ, van Delft JM, de Kok TM, et al.: Global gene expression analysis reveals differences in cellular responses to hydroxyl- and superoxide anion radical-induced oxidative stress in caco-2 cells. *Toxicol Sci* 2010;114:193–203.
34. Donato MT, Martinez-Romero A, Jimenez N, et al.: Cytometric analysis for drug-induced steatosis in HepG2 cells. *Chem Biol Interact* 2009;181:417–423.
35. Raja K, Thung SN, Fiel MI, Chang C: Drug-induced steatohepatitis leading to cirrhosis: long-term toxicity of amiodarone use. *Semin Liver Dis* 2009;29:423–428.
36. Antherieu S, Rogue A, Fromenty B, Guillouzo A, Robin MA: Induction of vesicular steatosis by amiodarone and tetracycline is associated with up-regulation of lipogenic genes in HepaRG cells. *Hepatology* 2011;53:1895–1905.

Address correspondence to:

Ivan Rusyn, MD, PhD

Department of Veterinary Integrative Biosciences
College of Veterinary Medicine and Biomedical Sciences

Texas A&M University

4458 TAMU

College Station, TX 77843

E-mail: irusyn@cvm.tamu.edu

Abbreviations Used

CV	=	coefficient of variation
DMSO	=	dimethyl sulfoxide
GPCR	=	G-protein-coupled receptor
HCS	=	high-content screening
HTS	=	high-throughput screening
iPSC	=	induced pluripotent stem cell
KRBG	=	Krebs-Ringer bicarbonate buffer
PBS	=	phosphate-buffered saline
POD	=	point-of-departure
ROS	=	reactive oxygen species
TAB	=	tetraoctylammonium bromide.